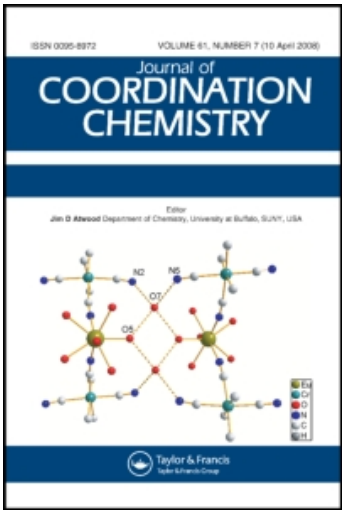

Journal of Coordination Chemistry
Publication details, including instructions for authors and subscription information:
http://www.informaworld.com/smpp/title~content=t713455674

A cobalt(II) coordination polymer with mixed 4-(5-mercapto-1*H*-tetrazol-1-yl)benzoate and 4,4'-bipyridine ligands: synthesis, crystal structure, and magnetic properties

Chun-Sen Liu[a]; E. Carolina sañudo[b]; Min Hu[a]; Qiang Zhang[a]; Liang-Qi Guo[a]; Shao-Ming Fang[a]
[a] Henan Provincial Key Laboratory of Surface and Interface Science, Zhengzhou University of Light Industry, Zhengzhou, Henan 450002, P.R. China [b] Institut de Nanociència i Nanotecnologia i Departament de Química Inorgànica, Universitat de Barcelona, Diagonal, 647, 08028 Barcelona, Spain

First published on: 04 September 2010

To cite this Article Liu, Chun-Sen , Carolina sañudo, E. , Hu, Min , Zhang, Qiang , Guo, Liang-Qi and Fang, Shao-Ming(2010) 'A cobalt(II) coordination polymer with mixed 4-(5-mercapto-1*H*-tetrazol-1-yl)benzoate and 4,4'-bipyridine ligands: synthesis, crystal structure, and magnetic properties', Journal of Coordination Chemistry, 63: 19, 3393 — 3402, First published on: 04 September 2010 (iFirst)
To link to this Article: DOI: 10.1080/00958972.2010.514337
URL: http://dx.doi.org/10.1080/00958972.2010.514337

Journal of Coordination Chemistry
Vol. 63, No. 19, 10 October 2010, 3393–3402

Taylor & Francis
Taylor & Francis Group

A cobalt(II) coordination polymer with mixed 4-(5-mercapto-1*H*-tetrazol-1-yl)benzoate and 4,4′-bipyridine ligands: synthesis, crystal structure, and magnetic properties

CHUN-SEN LIU*†, E. CAROLINA SAÑUDO*‡, MIN HU†, QIANG ZHANG†, LIANG-QI GUO† and SHAO-MING FANG*†

†Henan Provincial Key Laboratory of Surface and Interface Science, Zhengzhou University of Light Industry, Zhengzhou, Henan 450002, P.R. China
‡Institut de Nanociència i Nanotecnologia i Departament de Química Inorgànica, Universitat de Barcelona, Diagonal, 647, 08028 Barcelona, Spain

(*Received 23 March 2010; in final form 23 June 2010*)

A Co^{II} coordination polymer, $\{[Co(\mathbf{L})(bipy)(H_2O)_2](H_2O)_2\}_\infty$ (**1**), with 4-(5-mercapto-1*H*-tetrazol-1-yl)benzoate (**L**) and 4,4′-bipyridine (bipy), was synthesized and structurally characterized by single-crystal X-ray diffraction analysis. Complex **1** has a (4,4) 2-D network structure, which is further interlinked by inter-layer O–H $\cdots$ O hydrogen-bonding interactions to form a 2-fold interpenetrated binodal (3,5)-connected 3-D hydrogen-bonded $(6^3)(6^8 \cdot 8^2)$ topology. The magnetic properties of **1** feature weak antiferromagnetic coupling.

Keywords: Co^{II} complex; 4-(5-Mercapto-1*H*-tetrazol-1-yl)benzoic acid; Crystal structure; 2-Fold interpenetration; Magnetic properties

1. Introduction

Metal–organic frameworks (MOFs) have fascinating molecular and/or supramolecular structures and enormous potential applications in luminescence, magnetism, nonlinear optics, and gas storage [1]. Several strategies have been developed to control assembly of crystalline systems with desired structures and properties; choice of well-designed organic ligands as bridges or terminal groups and metal ions or clusters as nodes is one of the most effective ways. Appropriate choice of well-designed organic ligands is of importance in construction of MOFs because of variation in flexibility, length, and symmetry [2]. Carboxylic acids exhibiting diverse coordination, especially benzene-based carboxylic acids, have been employed in the preparation of metal–organic coordination complexes [3]. Ligands containing tetrazolate have also been used extensively to construct functional complexes due to their aromaticity and multiple N-donors [4]. The combinations of various coordination modes of tetrazolyl and carboxylate in tetrazolyl–carboxylate ligands may result in richer coordination modes for constructing new functional coordination polymers with unusual topologies [5].

*Corresponding authors. Email: chunsenliu@zzuli.edu.cn; carolina.sanudo@qi.ub.es; smfang@zzuli.edu.cn

Journal of Coordination Chemistry
ISSN 0095-8972 print/ISSN 1029-0389 online © 2010 Taylor & Francis
DOI: 10.1080/00958972.2010.514337

Metal complexes with heterocyclic thiones have been widely studied because of their relevance to biological systems and versatility in coordination [6]. However, the investigation of 5-mercapto-substituted tetrazoles has been less common. 4,4′-Bipyridyl-like linear bridging molecules as spacers into reaction systems involving various carboxylic acids, as auxiliary co-ligands, may generate interesting coordination architectures [7]. Magnetic properties of coordination polymers are of interest to their potential application as materials [8].

We selected 4-(5-mercapto-1*H*-tetrazol-1-yl)benzoic acid (H_2**L**) to construct new functional coordination complexes and report the synthesis and structure of one Co^{II} polymer of 4-(5-mercapto-1*H*-tetrazol-1-yl)benzoate (**L**) and 4,4′-bipyridine (bipy). The magnetic properties of **1** were also investigated.

2. Experimental

2.1. *General methods*

All starting reagents and solvents were commercially available and used as received. IR spectra were measured on a TENSOR 27 (Bruker) FT-IR spectrometer with KBr pellets from 4000 to 400 cm^{-1}. Elemental analyses of C, H, and N were performed on a Vario EL III elemental analyzer. The powder X-ray diffraction (PXRD) was recorded on a Rigaku D/Max-2500 diffractometer at 40 kV, 30 mA for a Cu-target tube and a graphite monochromator. The intensity data were recorded by continuous scan in a $2\theta/\theta$ mode from 3° to 80° with a step size of 0.02° and a scan speed of 8° min^{-1}. Simulation of PXRD spectra was carried out by the single-crystal data and diffraction-crystal module of the commercially available Cerius2 program [9]. Thermogravimetric analysis (TGA) was carried out on a Perkin-Elmer Diamond SII thermal analyzer from room temperature to 800°C under N_2 at a heating rate of 10°C min^{-1}. Variable-temperature magnetic susceptibilities were measured in "Servei de Magnetoquímica (Universitat de Barcelona)" on polycrystalline samples (*ca* 30 mg) with a Quantum Design MPMS SQUID magnetometer operating at a magnetic field of 5 T between 2 and 300 K. Diamagnetic corrections were evaluated from Pascal's constants for all constituent atoms. Magnetization measurements were carried out at low temperature (2 K) in the 0–5 T range.

2.2. *Synthesis of 1*

A mixed solution of 4-(5-mercapto-1*H*-tetrazol-1-yl)benzoic acid (H_2**L**) (0.05 mmol) and 4,4′-bipyridine (bipy) (0.05 mmol) in CH_3OH (10 mL), in the presence of excess 2,6-dimethylpyridine (*ca* 0.05 mL for adjusting the pH to basic), was carefully layered onto a H_2O solution (15 mL) of $Co(ClO_4)_2 \cdot 6H_2O$ (0.05 mmol) in a test tube. Wine-colored single crystals suitable for X-ray analysis were observed at the tube wall after *ca* 3 weeks. Yield: ~40% based on H_2**L**. Anal. Calcd for $C_{18}H_{20}CoN_6O_6S$: C, 42.61%; H, 3.97%; N, 16.56%. Found: C, 42.42%; H, 3.81%; N, 16.68%. IR (KBr pellet, cm^{-1}): 3447(s, br), 1928(w), 1757(w), 1605(s), 1546(s), 1413(m), 1363(vs), 1279(m), 1218(w), 1173(w), 1130(w), 1103(w), 1069(w), 1040(w), 1007(w), 961(w), 850(m), 817(s), 787(m), 732(m), 699(w), 633(m), 580(w), 462(w).

Table 1. Crystallographic data and structure refinement for **1**.

Empirical formula	$C_{18}H_{20}CoN_6O_6S$
Formula weight	507.39
Crystal system	Triclinic
Space group	$P\bar{1}$
Unit cell dimensions (Å, °)	
a	6.907(2)
b	11.426(4)
c	13.192(4)
α	89.135(4)
β	86.520(4)
γ	84.900(4)
Volume (Å^3), Z	1035.0(5), 2
Calculated density (g cm^{-3})	1.628
Absorption coefficient (mm^{-1})	0.981
F (000)	522
Crystal size (mm^3)	$0.37 \times 0.12 \times 0.09$
θ range for data collection (°)	2.35–25.00
Reflections collected	7634
Independent reflection	3623 [R(int) = 0.0407]
Max. and min. transmission	0.9169 and 0.7130
Data/restraints/parameters	3623/0/289
Goodness-of-fit on F^2	1.022
Final R indices [$I > 2\sigma(I)$]	$R_1{}^a = 0.0667$, $wR_2{}^b = 0.1741$
R indices (all data)	$R_1{}^a = 0.0891$, $wR_2{}^b = 0.1949$
Largest difference peak and hole (e Å^{-3})	1.752 and −0.759

[a] $R_1 = \Sigma(||F_o| - |F_c||)/\Sigma|F_o|$.
[b] $wR_2 = [\Sigma w(|F_o|^2 - |F_c|^2)^2/\Sigma w(F_o^2)^2]^{1/2}$.

Caution! Although we have not met with any problems in handling perchlorate salts during this study, these should be treated cautiously because of their potential explosive nature.

2.3. *Crystal structure determination*

X-ray single-crystal diffraction data for **1** were collected on a Bruker Smart 1000 CCD area-detector diffractometer at 294(2) K with Mo-Kα radiation (λ = 0.71073 Å) by ω scan mode. SAINT [10] was used for integration of the diffraction profiles. Semi-empirical absorption corrections were applied using SADABS. The structure was solved by direct methods using the SHELXS program of the SHELXTL package and refined by full-matrix least-squares methods with SHELXL [11]. The non-hydrogen atoms were refined anisotropically and hydrogens were added according to theoretical models. Crystallographic data and experimental details for structural analyses are summarized in table 1; selected bond lengths and angles as well as hydrogen-bonding geometries are listed in tables 2 and 3.

3. Results and discussion

3.1. *Crystal structure of 1*

Single-crystal X-ray diffraction reveals that **1** consists of (4,4) 2-D neutral layers and lattice water with one crystallographically unique cobalt (figure 1). Each asymmetric

Table 2. Selected bond distances (Å) and angles (°) for **1**.

Co(1)–O(1W)	2.060(3)	Co(1)–N(3)	2.232(4)
Co(1)–O(2W)	2.102(3)	Co(1)–S(1)$^{\#2}$	2.5128(15)
Co(1)–N(1)	2.152(4)	Co(1)–N(2)$^{\#1}$	2.156(4)
O(1W)–Co(1)–O(2W)	87.70(14)	O(1W)–Co(1)–S(1)$^{\#2}$	93.56(10)
O(1W)–Co(1)–N(1)	91.13(15)	O(2W)–Co(1)–S(1)$^{\#2}$	178.72(10)
O(2W)–Co(1)–N(1)	87.39(14)	N(1)–Co(1)–S(1)$^{\#2}$	92.38(11)
O(1W)–Co(1)–N(2)$^{\#1}$	91.39(15)	N(2)$^{\#1}$–Co(1)–S(1)$^{\#2}$	91.30(11)
O(2W)–Co(1)–N(2)$^{\#1}$	88.87(14)	N(3)–Co(1)–S(1)$^{\#2}$	88.69(11)
N(1)–Co(1)–N(2)$^{\#1}$	175.40(15)	O(1W)–Co(1)–N(3)	177.21(14)
O(2W)–Co(1)–N(3)	90.05(14)	N(1)–Co(1)–N(3)	90.41(15)
N(2)$^{\#1}$–Co(1)–N(3)	86.92(14)		

Symmetry codes for **1**: $^{\#1}x, y+1, z$; $^{\#2}x-1, y, z$; $^{\#3}x, y-1, z$; $^{\#4}x+1, y, z$.

Table 3. Selected hydrogen-bonding geometry (Å, °) for **1**.

D–H···A	*d*(D–H)	*d*(H···A)	*d*(D···A)	∠DHA
O(1W)–H(1WA)···O(2)^{a}	0.850	2.031	2.767(6)	144
O(1W)–H(1WB)···N(4)^{b}	0.851	2.241	2.897(8)	134
O(2W)–H(2WA)···O(3)	0.850	2.123	2.646(8)	119
O(2W)–H(2WA)···O(4)	0.850	2.331	2.681(7)	105
O(3W)–H(3WA)···O(1)^{c}	0.850	1.878	2.728(6)	179
O(3W)–H(3WB)···O(1)^{d}	0.849	1.989	2.835(9)	174
O(4W)–H(4WA)···O(2)^{e}	0.849	1.875	2.718(6)	171
O(4W)–H(4WB)···O(2)^{d}	0.850	2.134	2.809(8)	136
C(13)–H(13A)···O(4W)^{f}	0.929	2.550	3.234(9)	131
C(15)–H(15A)···S(1)^{c}	0.930	2.816	3.643(8)	149

Symmetry codes for **1**: $^{a}x-1, y, z+1$; $^{b}x-1, y, z$; $^{c}-x+2, -y, -z$; $^{d}x, y, z+1$; $^{e}-x+2, 1-y, -z$; $^{f}-x+1, -y, 1-z$.

unit contains one Co^{II}, one 4-(5-mercapto-1*H*-tetrazol-1-yl)benzoate (**L**), one bridging 4,4′-bipyridine (bipy), two coordinated water molecules, and two lattice water molecules. The Co(1) is in a distorted octahedral geometry, coordinated by two nitrogens from bipy, one nitrogen and one sulfur from two different **L**, and two H_2O (figure 1a and figure S1 in "Supplementary material"). All the Co–O bond distances [2.152(4)–2.232(4) Å], Co–N [2.060(3)–2.102(3) Å], and Co–S [2.5128(15) Å] as well as bond angles around Co^{II} [87.39(14)–178.72(10)°] (table 1) are in the range expected for similar complexes [6c, 12]. Each **L** bridges adjacent Co^{II}'s to yield a 1-D zig–zag chain with a non-bonding Co···Co separation of 6.9072(2) Å. Bipy serves as a linear bridging spacer with a head-to-end mode [N(1)–Co(1)–N(2)$^{\#1}$: 175.40(15)°; symmetry code for $^{\#1} = x, y+1, z$]. Such linkages lead to a (4,4) 2-D network structure running parallel to the (0 0 1) plane (figure 1a). O(1W) of coordinated H_2O presents strong intra-layer hydrogen-bonding interactions with the uncoordinated N(4) of **L** [O(1W)···N(4): 2.8974(6) Å; O(1W)–H(1WA)···N(4): 134°) (see figure 1a and table 3 as well as figure S1 in the "Supplementary material").

The combination of coordination chemistry with non-covalent interactions, such as hydrogen bonding, provides a powerful method for creating higher dimensional supramolecular architectures from simple building blocks [13]. In **1**, adjacent 2-D layers are further assembled into a 3-D supramolecular framework by the inter-layer O–H···O hydrogen-bonding interactions between the carboxylate O atoms of **L** and coordinated water (O(1W)–H(1W)···O(2)^{a}, symmetry code for $^{a} = x-1, y, z+1$; see

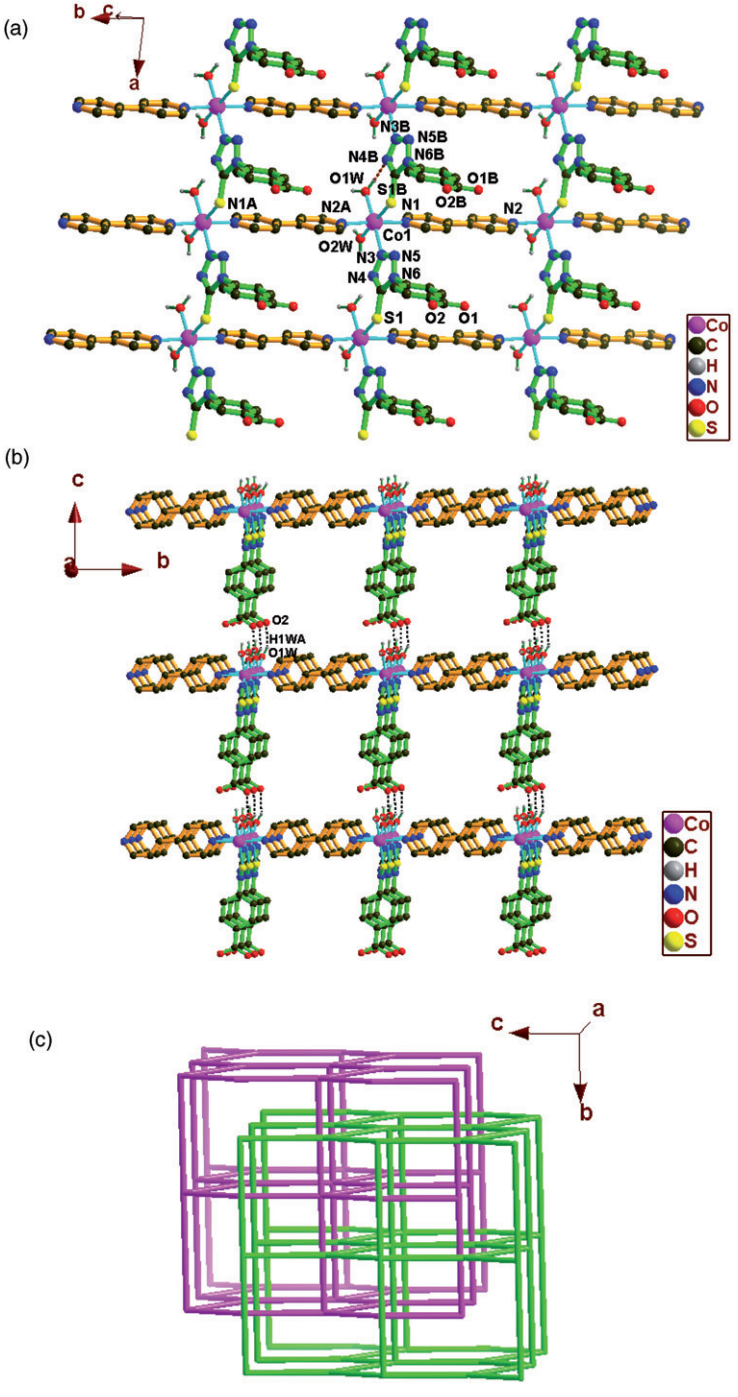

Figure 1. View of: (a) the (4,4) 2-D network, showing the local coordination environment of Co^{II} in **1** and the intra-layer O–H $\cdots$ O hydrogen-bonding interactions (red dashed lines); (b) the 3-D framework, along the [100] direction, formed by the inter-layer O–H$\cdots$O interactions (black dashed lines); and (c) a schematic representation of the binodal (3,5)-connected 2-fold interpenetrated 3-D hydrogen-bonded topological network with the Schläfli symbol $(6^3)(6^8 \cdot 8^2)$. The symmetry-related atoms labeled with the suffixes A and B are generated by the symmetry operations $(x, y+1, z)$ and $(x-1, y, z)$, respectively. For clarity, lattice water molecules were omitted and only hydrogens involved in interactions are shown.

table 3) (figure 1b). Complicated structures usually can be broken down into simple networks of nodes and links, facilitating easier and quicker understanding of connectivity between the components of the crystal structures [14]. To describe the overall 3-D framework, it is best to reduce **1** to its underlying topological network. Considering the inter-layer O–H···O hydrogen-bonding interactions between **L** and coordinated water, each **L** coordinates to three metal ions as a planar three-connecting node; bipy connects to only two metals and can be ignored topologically – it just forms a link. Each Co^{II} connects to three **L** and two bipy, acting as a five-connecting node. The resulting binodal (3,5)-connected 3-D hydrogen-bonded topological network has the Schläfli symbol of $(6^3)(6^8 \cdot 8^2)$ (representing **L** and Co^{II} nodes, respectively) (see figure S2 in "Supplementary material") [15]. The 3-D hydrogen-bonded motifs are intertwined into a 2-fold interpenetrated network to further stabilize the framework of **1** (figure 1c). Such interpenetration in hydrogen-bonded networks has been far less common than valence-bonded ones (MOFs) [16].

The structure of **1** also contains $\pi \cdots \pi$ stacking interactions between the pyridine and phenyl rings in a face-to-face fashion with the centroid–centroid separation of 3.6914 Å as well as C–H···S hydrogen-bonding interactions between S and pyridine of **L** and bipy (C(15)–H(15A)···S(1)^c, symmetry code for $^c = -x+2, -y, -z$; see table 3). Finally, lattice water molecules were included within the void space of the framework in **1**, forming O–H···O and C–H···O hydrogen-bonding interactions with **L** and coordinated water (table 3). These O–H···O, O–H···N, C–H···O, and C–H···S hydrogen bonds as well as $\pi \cdots \pi$ stacking interactions were checked and calculated by PLATON procedure [17].

3.2. *PXRD result of 1*

To confirm whether the crystal structures are truly representative of the bulk materials, PXRD experiments have been carried out for **1**. The PXRD experimental and computer-simulated patterns of **1** are shown in figure 2. Although the experimental patterns have a few unindexed diffraction lines and some are slightly broadened in comparison with those simulated from the single-crystal modes, it still can be considered that the bulk synthesized materials and the as-grown crystals are homogeneous for **1**.

3.3. *Magnetic properties of 1*

Susceptibility data measured in the 300–2 K temperature range are shown in figure 3 as χ and χ_T *versus* T plots. At an applied field of 5000 G, the χ_T product has a value of 3.31 $cm^3\,K\,mol^{-1}$ at 300 K. As temperature decreases, so does the χ_T product, to a value of 1.39 $cm^3\,K\,mol^{-1}$ at 2 K; this is due to depopulation of the $J = 5/2$ state and population of the $J = ½$ state, as well as to antiferromagnetic coupling between the Co^{II} ions of **1**. The high temperature data from 20 to 300 K can be fitted to the Curie–Weiss law with a Curie constant $C = 3.49\,cm^3\,mol^{-1}$ and a Weiss constant $\theta = -15.57$ K ($r = 0.998$), in agreement with antiferromagnetic coupling. At 2 K, the reduced magnetization ($M/N\mu_B$) (figure S3 in "Supplementary material") shows an increase with field, to the highest value of 2.4 at 5 T, which is in agreement with a Co^{II} with strong unquenched spin–orbit coupling. All the data are consistent with a Co^{II} in an

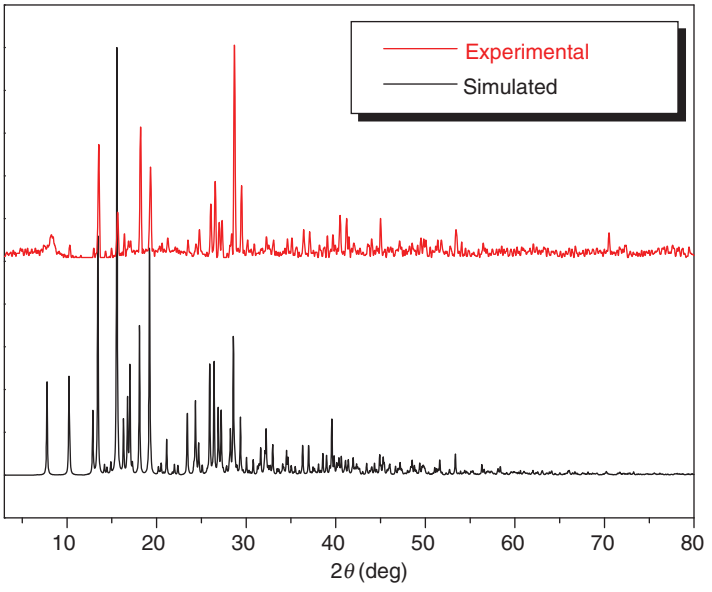

Figure 2. PXRD pattern of **1**.

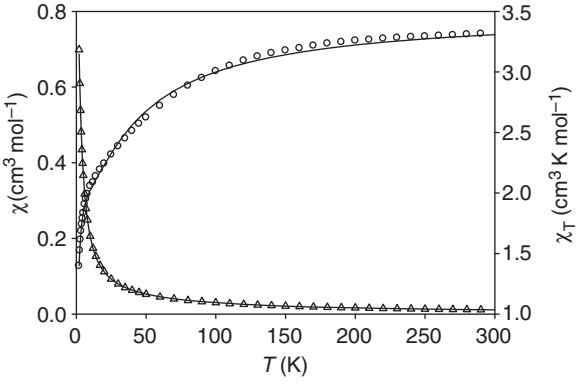

Figure 3. Susceptibility data for **1**, shown as χ (triangles) and χ_T (circles) *vs.* T plots at 5000 G applied field. The solid line is the best fit using a phenomenological equation that takes into account the spin–orbit coupling for Co^{II}; see text for fitting parameters.

octahedral environment with unquenched orbital momentum. There is no zero-field cool–field cool (ZFC–FC) hysteresis at 50 G and no long-range order, shown by the absence of a signal in the AC magnetic susceptibility. There is no available analytical expression to model the susceptibility of 1-D and 2-D Co^{II} compounds with unquenched orbital momentum as in **1**. However, the order of the weak antiferromagnetic coupling can be estimated using the phenomenological equation $\chi_T = A\exp(-E_{SOC}/kT) + B\exp(-E_{AF}/kT)$ [18], where $A + B$ equals the Curie constant and E_{SOC} and E_{AF} represent the "activation energies" corresponding to the spin–orbit coupling and antiferromagnetic exchange interaction, respectively. The obtained values are in agreement with the Curie–Weiss fitting of the high-temperature data (20–300 K)

since $C = 3.49\,cm^3\,mol^{-1}$ and $A + B = 3.5\,cm^3\,mol^{-1}$ ($A = 1.3$ and $B = 2.2$) (figure S4 in the "Supplementary material"). The obtained $E_{SOC}/k = 56\,K$ is in agreement with reported values for Co^{II} [19]. Taking the anisotropic Ising spin approximation at low temperatures, $J = 2E_{AF}/k = -1.9\,K$, the best fitting is shown in figure 3 as a solid line. Even though this is a very simple phenomenological model, it describes adequately the spin–orbit coupling, which results in a splitting between discrete levels, and the exponential low-temperature divergence of the susceptibility [$\chi_T \sim \exp(\alpha J/2kT)$].

The observed magnetic behavior is consistent with the crystal structure of **1**, which consists of zig–zag chains of Co^{II} bridged by **L** and linked into layers by bipy. Although there are many examples of Co^{II} 1-D and 2-D networks with 4,4′-bipyridine (bipy) [20], in most cases magnetic properties are not analyzed due to the difficulty posed by the strong spin–orbit coupling of Co^{II} which precludes a quantitative analysis. However, in many cases, analyses of magnetic properties similar to the one reported here are performed, and in all cases, similar conclusions are achieved: the coupling through 4,4′-bipyridine is weak and antiferromagnetic [12a, 21]. This is similar to what happens with other transition metals, for example Cu^{II}, where 4,4′-bipyridine is known to mediate antiferromagnetic coupling of $<2\,cm^{-1}$ [22]. As can be observed in the crystal structure, the aromatic rings of bipy are coplanar facilitating the antiferromagnetic exchange between Co^{II} ions.

3.4. *TGA of 1*

To examine the thermal stabilities of **1**, TGA of the crystalline material was performed from room temperature to 800°C with a heating rate of $10°C\,min^{-1}$ under nitrogen (figure 4). The TGA curve of **1** shows the first weight loss of 13.95% between 30°C and 110°C (peaking at 102°C), which can be attributed to loss of lattice and coordinated water (calculated, 14.20%). Then the mass remained largely unchanged until the decomposition onset at 230°C. The framework of **1** decomposed quickly in one big step peaking at 284°C with a weight loss of 30.64% from 230°C to 340°C, very close to the

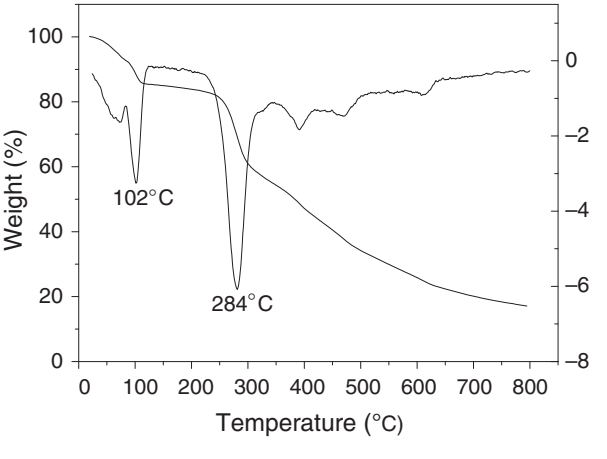

Figure 4. TGA plots for **1**.

calculated value of 30.78% corresponding to components of bipy. The final residue is not characterized because its weight loss does not stop until heating ends at 800°C.

4. Conclusions

We have obtained a new 2-D Co^{II} coordination polymer, $\{[Co(\mathbf{L})(bipy)(H_2O)_2](H_2O)_2\}_\infty$, using 4-(5-mercapto-1*H*-tetrazol-1-yl)benzoic acid ($H_2\mathbf{L}$) and 4,4′-bipyridine (bipy). The magnetic properties of **1** have been investigated in detail, exhibiting weak antiferromagnetic coupling. The procedures described here might be generally applicable for d^{10} transition metal ions, such as Ag^{I}, Zn^{II}, and Cd^{II}, to construct other metal–organic coordination complexes with potential properties. Further efforts on this perspective are underway in our laboratory.

Supplementary material

Additional figures and plots of magnetization data for **1** and crystallographic data (excluding structure factors) for the crystal structure reported in this article have been deposited with the Cambridge Crystallographic Data Centre and allocated the deposition number: CCDC 769421. This material can be obtained free of charge *via* www.ccdc.cam.ac.uk/conts/retrieving.html or from the CCDC, 12 Union Road, Cambridge CB2 1EZ, UK; Fax: +44 1223 336033; Email: deposit@ccdc.cam.ac.uk.

Acknowledgments

This study was supported by the National Natural Science Fund of China (Grant Nos. 20801049 and 20771095) and the Startup Fund for PhDs of Natural Scientific Research of Zhengzhou University of Light Industry (Grant No. 2007BSJJ001 to CSL). ECS acknowledges the financial support from the Spanish Government (Grant CTQ2009-06959 and Ramón y Cajal contract). We also thank Mr X.-G. Yang for helping us to discuss the topology of **1**.

References

[1] (a) Z. Wang, S.M. Cohen. *Chem. Soc. Rev.*, **38**, 1315 (2009); (b) R.J. Kuppler, D.J. Timmons, Q.-R. Fang, J.-R. Li, T.A. Makal, M.D. Young, D. Yuan, D. Zhao, W. Zhuang, H.-C. Zhou. *Coord. Chem. Rev.*, **253**, 3042 (2009); (c) Y.-T. Wang, G.-M. Tang, Y.-Q. Wei, T.-X. Qin, T.-D. Li, C. He, J.-B. Ling, X.-F. Long, S.W. Ng. *Cryst. Growth Des.*, **10**, 25 (2010); (d) J.-P. Zhao, B.-W. Hu, E.C. Sañudo, Q. Yang, Y.-F. Zeng, X.-H. Bu. *Inorg. Chem.*, **48**, 2482 (2009).

[2] (a) G. Férey. *Chem. Soc. Rev.*, **37**, 191 (2008); (b) H. Lin, P. A. Maggard. *Cryst. Growth Des.*, **10**, 1323 (2010); (c) Z. Guo, G. Li, L. Zhou, S. Su, Y. Lei, S. Dang, H. Zhang. *Inorg. Chem.*, **48**, 8069 (2009).

[3] (a) F.B. Johansson, A.D. Bond, C.J. McKenzie. *Inorg. Chem.*, **46**, 2224 (2007); (b) K.S. Gavrilenko, Y. Le Gal, O. Cador, S. Golhen, L. Ouahab. *Chem. Commun.*, 280 (2007); (c) K.S. Gavrilenko, O. Cador, K. Bernot, P. Rosa, R. Sessoli, S. Golhen, V.V. Pavlishchuk, L. Ouahab. *Chem. Eur. J.*, **14**, 2034 (2008); (d) T.C. Stamatatos, A.K. Boudalis, K.V. Pringouri, C.P. Raptopoulou, A. Terzis, J. Wolowska, E.J.L. McInnes, S.P. Perlepes. *Eur. J. Inorg. Chem.*, 5098 (2007).
[4] (a) W. Yang, X. Lin, A.J. Blake, C. Wilson, P. Hubberstey, N.R. Champness, M. Schroder. *CrystEngComm*, **11**, 67 (2009); (b) T.M. Klapotke, C.M. Sabate, M. Rasp. *Dalton Trans.*, 1825 (2009); (c) J.-M. Lin, B.-S. Huang, Y.-F. Guan, Z.-Q. Liu, D.-Y. Wang, W. Dong. *CrystEngComm*, **11**, 329 (2009); (d) M. Li, Z. Li, D. Li. *Chem. Commun.*, 3390 (2008).
[5] (a) Y. Li, G. Xu, W.-Q. Zou, M.-S. Wang, F.-K. Zheng, M.-F. Wu, H.-Y. Zeng, G.-C. Guo, J.-S. Huang. *Inorg. Chem.*, **47**, 7945 (2008); (b) Z.-P. Yu, S.-S. Xiong, G.-P. Yong, Z.-Y. Wang. *J. Coord. Chem.*, **62**, 242 (2009); (c) T. Jiang, Y.-F. Zhao, X.-M. Zhang. *Inorg. Chem. Commun.*, 1194 (2007).
[6] (a) Y.-J. Kim, J.-T. Han, S. Kang, W.S. Han, S.W. Lee. *Dalton Trans.*, 3357 (2007); (b) K. Fujisawa, T. Kakizaki, Y. Miyashita, K. Okamoto. *Inorg. Chim. Acta*, **361**, 1134 (2008); (c) S.M. Humphrey, J.-S. Chang, S.H. Jhung, J.W. Yoon, P.T. Wood. *Angew. Chem. Int. Ed.*, **46**, 272 (2007).
[7] (a) W.-T. Chen, M.-S. Wang, X. Liu, G.-C. Guo, J.-S. Huang. *Cryst. Growth Des.*, **6**, 2289 (2006); (b) R. Wang, X. Wang, E.B. Sundberg, P. Nguyen, G.P.G. Grant, C. Sheth, Q. Zhao, S. Herron, K.A. Kantardjieff, L. Li. *Inorg. Chem.*, **48**, 9779 (2009).
[8] (a) D. Sarma, K.V. Ramanujachary, S.E. Lofland, T. Magdaleno, S. Natarajan. *Inorg. Chem.*, **48**, 11660 (2009); (b) X. Li, B. Wu, R. Wang, H. Zhang, C. Niu, Y. Niu, H. Hou. *Inorg. Chem.*, **49**, 2600 (2010).
[9] *Cerius2*. Molecular Simulation Inc., San Diego, CA (2001).
[10] Bruker AXS. *SAINT Software Reference Manual*, Bruker AXS Inc., Madison, WI (1998).
[11] G.M. Sheldrick. *SHELXTL NT Version 5.1, Program for Solution and Refinement of Crystal Structures,* University of Göttingen, Germany (1997).
[12] (a) L.-F. Ma, L.-Y. Wang, Y.-Y. Wang, S.R. Batten, J.-G. Wang. *Inorg. Chem.*, **48**, 915 (2009); (b) I.L. Malaestean, M. Speldrich, S.G. Baca, A. Ellern, H. Schilder, P. Kogerler. *Eur. J. Inorg. Chem.*, 1011 (2009).
[13] (a) G.-L. Wen, Y.-Y. Wang, W.-H. Zhang, C. Ren, R.-T. Liu, Q.-Z. Shi. *CrystEngComm*, **12**, 1238 (2010); (b) G.R. Desiraju. *Acc. Chem. Res.*, **35**, 565 (2002).
[14] S.R. Batten, S.M. Neville, D.R. Turner, *Coordination Polymers Design, Analysis and Application*, The Royal Society of Chemistry, Cambridge (2009).
[15] (a) G.R. Desiraju, T. Steiner, *The Weak Hydrogen Bond in Structural Chemistry and Biology*, Oxford University Press, Oxford (1999); (b) P. Hobza, Z. Havlas. *Chem. Rev.*, **100**, 4253 (2000).
[16] (a) X.-L. Wang, C. Qin, E.-B. Wang, Z.-M. Su. *Chem. Eur. J.*, **12**, 2680 (2006); (b) T. Wu, M. Li, D. Li, X.-C. Huang. *Cryst. Growth Des.*, **8**, 568 (2008); (c) L. Zhang, Y.-L. Yao, Y.-X. Che, J.-M. Zheng. *Cryst. Growth Des.*, **10**, 528 (2010).
[17] (a) A.L. Spek, PLATON, *A Multipurpose Crystallographic Tool*, Utrecht University, Utrecht, The Netherlands, 2005, available online at: http://www.cryst.chem.uu.nl/platon (for Unix) and http://www.chem.gla.ac.uk/~louis/software/platon/ (for MS Windows); (b) H. Küppers, F. Liebau, A.L. Spek. *J. Appl. Crystallogr.*, **39**, 338 (2006).
[18] J.-M. Rueff, N. Masciocchi, P. Rabu, A. Sironi, A. Skoulios. *Eur. J. Inorg. Chem.*, 2843 (2001).
[19] R.L. Carlin. *Magnetochemistry*, Heidelberg, Springer-Verlag, Berlin (1986).
[20] (a) M. Felloni, A.J. Blake, N.R. Champness, P. Hubberstey, C. Wilson, M. Schröder. *J. Supramol. Chem.*, **2**, 163 (2002); (b) S.W. Lee, H.J. Kim, Y.K. Lee, K. Park, J.-H. Son, Y.-U. Kwon. *Inorg. Chim. Acta*, **353**, 151 (2003).
[21] (a) R. Fu, S. Hu, X. Wu. *Inorg. Chem.*, **46**, 9630 (2007); (b) D.-X. Xue, W.-X. Zhang, X.-M. Chen. *J. Mol. Struct.*, **877**, 36 (2008); (c) L.-M. Zheng, X. Fang, K.-H. Lii, H.-H. Song, X.-Q. Xin, H.-K. Fun, K. Chinnakali, I.A. Razak. *J. Chem. Soc., Dalton Trans.*, 2311 (1999).
[22] M.S. Haddad, D.N. Hendrickson, J.P. Cannady, R.S. Drago, D.S. Bieksza. *J. Am. Chem. Soc.*, **101**, 898 (1979).